Cell Reports

Report

T Follicular Helper Cells Promote a Beneficial Gut Ecosystem for Host Metabolic Homeostasis by Sensing Microbiota-Derived Extracellular ATP

Graphical Abstract

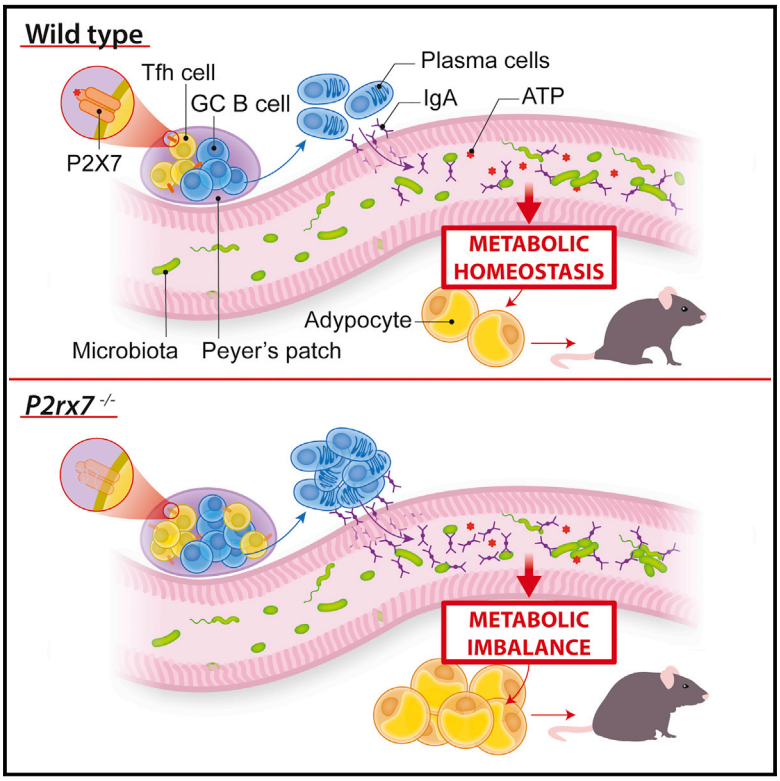

Highlights

- P2X7 receptor activity in Tfh cells is important for shaping the gut microbiota
- Control of secretory IgA by Tfh cells promotes a healthy gut ecosystem
- Lack of P2X7 in Tfh cells results in selection of an obesogenic microbiota
- Sensing of extracellular ATP by P2X7 in Tfh cells promotes host metabolic balance

Authors

Lisa Perruzza, Giorgio Gargari, Michele Proietti, ..., Kathy D. McCoy, Simone Guglielmetti, Fabio Grassi

Correspondence

fabio.grassi@irb.usi.ch

In Brief

Gut commensals contribute to host metabolic homeostasis. ATP released by bacteria limits IgA secretion in the small intestine via the P2X7 receptor expressed in T follicular helper cells. Perruzza et al. show that this regulatory mechanism is important for shaping a diverse microbiota that promote host metabolic homeostasis.

Perruzza et al., 2017, Cell Reports *18*, 2566–2575
March 14, 2017
http://dx.doi.org/10.1016/j.celrep.2017.02.061

CellPress

OPEN ACCESS
CellPress

Cell Reports
Report

T Follicular Helper Cells Promote a Beneficial Gut Ecosystem for Host Metabolic Homeostasis by Sensing Microbiota-Derived Extracellular ATP

Lisa Perruzza,[1,2] Giorgio Gargari,[3] Michele Proietti,[1,16] Bruno Fosso,[4] Anna Maria D'Erchia,[4,5] Caterina Elisa Faliti,[1,2] Tanja Rezzonico-Jost,[1] Daniela Scribano,[6,7] Laura Mauri,[8] Diego Colombo,[8] Giovanni Pellegrini,[9] Annalisa Moregola,[10] Catherine Mooser,[11] Graziano Pesole,[4,5] Mauro Nicoletti,[6] Giuseppe Danilo Norata,[10,12] Markus B. Geuking,[11,13] Kathy D. McCoy,[11,14] Simone Guglielmetti,[3] and Fabio Grassi[1,8,15,17,*]

[1]Institute for Research in Biomedicine, Università della Svizzera Italiana, 6500 Bellinzona, Switzerland
[2]Graduate School for Cellular and Biomedical Sciences, University of Bern, 3001 Bern 9, Switzerland
[3]Department of Food, Environmental, and Nutritional Sciences (DeFENS), Università degli Studi di Milano, 20133 Milan, Italy
[4]Institute of Biomembranes and Bioenergetics, National Research Council, 70126 Bari, Italy
[5]Department of Biosciences, Biotechnologies and Biopharmaceutics, University of Bari, 70126 Bari, Italy
[6]Department of Medical and Oral Sciences and Biotechnologies, University "Gabriele D'Annunzio", 66100 Chieti, Italy
[7]Departement of Public Health and Infectious Diseases, University "La Sapienza" of Rome, 00185 Rome, Italy
[8]Department of Medical Biotechnology and Translational Medicine (BIOMETRA), Università degli Studi di Milano, 20129 Milan, Italy
[9]Laboratory for Animal Model Pathology, Institute of Veterinary Pathology, Vetsuisse Faculty, University of Zurich, 8057 Zurich, Switzerland
[10]Department of Pharmacological and Biomolecular Sciences (DiSFeB), Università degli Studi di Milano, 20133 Milan, Italy
[11]Maurice Müller Laboratories, Universitätsklinik für Viszerale Chirurgie und Medizin (UVCM), University of Bern, 3010 Bern, Switzerland
[12]School of Biomedical Sciences, Curtin Health Innovation Research Institute, Curtin University, Perth, WA 6845, Australia
[13]Department of Microbiology, Immunology and Infectious Diseases and Calvin, Phoebe and Joan Snyder Institute for Chronic Diseases, Cumming School of Medicine, University of Calgary, Calgary, AB T2N 4N1, Canada
[14]Department of Physiology and Pharmacology and Calvin, Phoebe and Joan Snyder Institute for Chronic Diseases, Cumming School of Medicine, University of Calgary, Calgary, AB T2N 4N1, Canada
[15]Istituto Nazionale Genetica Molecolare "Romeo ed Enrica Invernizzi," 20122 Milan, Italy
[16]Present address: CCI-Center for Chronic Immunodeficiency, Universitätsklinikum Freiburg, 79106 Freiburg, Germany
[17]Lead Contact
*Correspondence: fabio.grassi@irb.usi.ch
http://dx.doi.org/10.1016/j.celrep.2017.02.061

SUMMARY

The ATP-gated ionotropic P2X7 receptor regulates T follicular helper (Tfh) cell abundance in the Peyer's patches (PPs) of the small intestine; deletion of *P2rx7,* encoding for P2X7, in Tfh cells results in enhanced IgA secretion and binding to commensal bacteria. Here, we show that Tfh cell activity is important for generating a diverse bacterial community in the gut and that sensing of microbiota-derived extracellular ATP via P2X7 promotes the generation of a proficient gut ecosystem for metabolic homeostasis. The results of this study indicate that Tfh cells play a role in host-microbiota mutualism beyond protecting the intestinal mucosa by induction of affinity-matured IgA and suggest that extracellular ATP constitutes an inter-kingdom signaling molecule important for selecting a beneficial microbial community for the host via P2X7-mediated regulation of B cell help.

INTRODUCTION

The gastrointestinal tract of mammals is colonized by bacteria at birth, and, thereafter, a mutualistic interaction with the evolving microbiota is established. The microbiota regulates the metabolic balance of the organism by generating bioactive molecules that are absorbed through the intestinal epithelium. A comparison of conventionally reared and germ-free (GF) mice showed that the gut microbiota regulates host fat storage. The transfer of cecal microbiota from conventional to GF mice results in a significant increase in body fat content and insulin resistance (Bäckhed et al., 2004). A primary role of intestinal commensals in the pathophysiology of metabolism was shown by reproduction of an obese phenotype in GF mice by transplantation of the microbiota isolated from obese animals (Turnbaugh et al., 2006).

Bacteria stimulate the development of gut-associated lymphoid tissue (GALT) (Macpherson and Harris, 2004). The intestinal tissue must integrate commensal bacteria and maintain their number and composition without inducing inflammation-mediated tissue damage (Littman and Pamer, 2011). Central in this homeostatic relationship is the production of immunoglobulin A (IgA). T follicular helper (Tfh) cells in the Peyer's patches (PPs) of the small intestine promote germinal center (GC) reactions and affinity maturation of IgA responses that are critical for efficient mucosal defense by limiting the translocation of potentially invasive bacteria and microbial inflammatory compounds from the gut lumen into the organism (Fagarasan et al., 2002; Shroff et al., 1995; Wei et al., 2011). Importantly, regulation of high-affinity IgA responses by T follicular regulatory (Tfr) cells

promotes the diversification and influences the composition of the microbiota in the gut (Kawamoto et al., 2014).

In mice deficient for the ATP-gated ionotropic receptor P2X7 (*P2rx7*$^{-/-}$), Tfh cells are significantly increased in PPs because of resistance to cell death induced by extracellular ATP. The altered regulation of Tfh cells in these mice results in enhanced secretory IgA responses (Proietti et al., 2014). Here we show that lack of P2X7-mediated control of Tfh cells results in altered microbiota composition that is responsible for impaired glucose homeostasis and enhanced fat deposition.

RESULTS

Increased Body Weight and Impaired Glucose Metabolism in *P2rx7*$^{-/-}$ Mice

A characteristic trait of *P2rx7*$^{-/-}$ mice is the increase in body weight with respect to wild-type (WT) littermates (Beaucage et al., 2014; Figure 1A). *P2rx7*$^{-/-}$ animals at 8 weeks had a significant increase in blood glucose, white adipose tissue (WAT) mass, serum insulin, and leptin with respect to WT littermates (Figures 1B–1D). Moreover, *P2rx7*$^{-/-}$ mice showed significant glucose intolerance and decreased insulin sensitivity, as measured by glucose tolerance test (GTT) and insulin tolerance test (ITT) (Figures 1E and 1F). Food consumption was not different between the two strains of mice (data not shown), as were plasma total cholesterol (76.9 ± 23.1 mg/dL versus 66.5 ± 17.5 mg/dL in 9-week-old WT and *P2rx7*$^{-/-}$ animals, respectively; n = 5) and plasma triglyceride levels (104.2 ± 25.4 mg/dL versus 95.4 ± 14.9 mg/dL in WT and *P2rx7*$^{-/-}$ animals, respectively).

Macroscopic analysis at 9 weeks revealed liver enlargement (weights, WT: 1.057 ± 0.04 g; *P2rx7*$^{-/-}$: 1.346 ± 0.038 g; n = 10; p = 0.0006) that was associated with significantly elevated glycogen in fasted *P2rx7*$^{-/-}$ compared with WT mice, which exhibited only minimal, scattered glycogen deposition (Figure S1A). Glucokinase (GCK) mRNA levels were significantly increased in *P2rx7*$^{-/-}$ mice, suggesting that hyperglycemia could result in increased glucose flux (Figure S1B). However, intracellular glucose does not appear to enter glycolysis because transcript levels of the key enzyme glyceraldehyde 3-phosphate dehydrogenase (GAPDH), which catabolizes the conversion of glucose 1,3 biphospate to 1,3-bisphosphoglyceric acid and fosters glycolysis, were reduced (Figure S1B). This implies that increased intracellular glucose could be accumulated as glycogen and, indeed, could explain the observed phenotype. Other metabolic pathways in the liver did not appear to be affected (Figure S1B). These results suggest that P2X7 activity is important in the regulation of glucose homeostasis. The altered metabolic control we observed in *P2rx7*$^{-/-}$ mice was worsened by a high-fat diet, which induced a significant increase in body and WAT weights as well as significantly impaired glucose tolerance and insulin sensitivity with respect to WT littermates (Figures S1C and S1D), suggesting that *P2rx7*$^{-/-}$ mice are more sensitive to increased caloric intake.

Altered Microbiota Composition in *P2rx7*$^{-/-}$ Mice

Hierarchical clustering of mice for cecal microbiota showed that *P2rx7*$^{-/-}$ animals clustered together and separately with respect to WT littermates (Figure 1G). Among the most represented families, we detected the increase of Lachnospiraceae and Helicobacteraceae in *P2rx7*$^{-/-}$ mice. In contrast, Paraprevotellaceae and Caulobacteraceae were enriched in WT animals (Figure 1H). The increase of Lachnospiraceae within gut commensals has been associated with obesity (Cho et al., 2012). Many species belonging to this family have been shown to produce butyrate (Duncan et al., 2002; Meehan and Beiko, 2014), the abundance of which has been associated with obesity (Cho et al., 2012; Turnbaugh et al., 2006). Quantification of short chain fatty acids (SCFAs) in cecal content of WT and *P2rx7*$^{-/-}$ mice revealed a significant increase in butyrate in mutant mice (Figure 1I). These data suggest that variations in selected families of the microbiota might result from deletion of *P2rx7* and contribute to the observed altered glucose metabolism.

Cell-Intrinsic Role of Tfh Cells in Glucose Homeostasis

Adoptive transfer of *P2rx7*$^{-/-}$ Tfh cells into lymphopenic mice results in enhanced expansion in PPs with respect to WT cells (Proietti et al., 2014; Figure S2A). 1 month after transfer into *Cd3e*$^{-/-}$ mice, both WT and *P2rx7*$^{-/-}$ cells maintained the Tfh phenotype, characterized by CXCR5, Bcl6, PD1, and inducible T-cell costimulator (ICOS) expression, with few cells expressing Foxp3 (Figures S2B–S2D). Transfer of mutant cells resulted in significantly enhanced GC reactions (Figure S2E), increased body and WAT weights, and increased blood glucose, insulin, and leptin levels (Figures 2A and 2B). GTT also revealed impaired glucose sensitivity (Figure 2C). Firmicutes were significantly increased, with concomitant reduction of both Bacteroidetes and Proteobacteria (Figure 2D). The analysis of variations in family abundances showed a significant increase in Lachnospiraceae, a characteristic feature of *P2rx7*$^{-/-}$ mice (Figure 1H), and of an undetermined family belonging to the order Clostridiales in *P2rx7*$^{-/-}$ chimeric mice (Figure 2E). Moreover, quantification of SCFAs showed a significant increase in butyrate (Figure 2F). Therefore, *P2rx7*$^{-/-}$ Tfh cells appear to be sufficient for determining the modifications in metabolic parameters and microbiota composition that were observed in *P2rx7*$^{-/-}$ mice.

Selective Role of Tfh Cells in Regulating Glucose Metabolism

To understand whether Tfh cell activity in *P2rx7*$^{-/-}$ mice played a causative role in the development of metabolic syndrome by shaping the microbiota, we compared *Icos*$^{-/-}$ and *Icos*$^{-/-}$ *P2rx7*$^{-/-}$ double mutant mice, which are devoid of Tfh and GC B cells (Figures S3A and S3B), for microbiota composition and metabolic parameters. *Icos*$^{-/-}$ mice exhibit normal CD4 and CD8 cell populations in lymph nodes and spleen (Dong et al., 2001). However, effector/memory CD4 (CD44^{+}CD62L^{-}) as well as T regulatory and Th17 cells in PPs and mesenteric lymph nodes (MLNs) were significantly reduced (Figures S3C and S3D). *Icos*$^{-/-}$ mice were characterized by an increase in IgA-coated bacteria in stools with respect to WT mice (Figure S4A), a finding consistent with a predominant T-independent IgA response to commensals (Bunker et al., 2015) and modulation of the secretory IgA response by Tfh cells (Kawamoto et al., 2014). Concomitant deletion of *P2rx7* did not affect IgA coating in ICOS-deficient mice, indicating that lack of P2X7 in ICOS^{-} cells

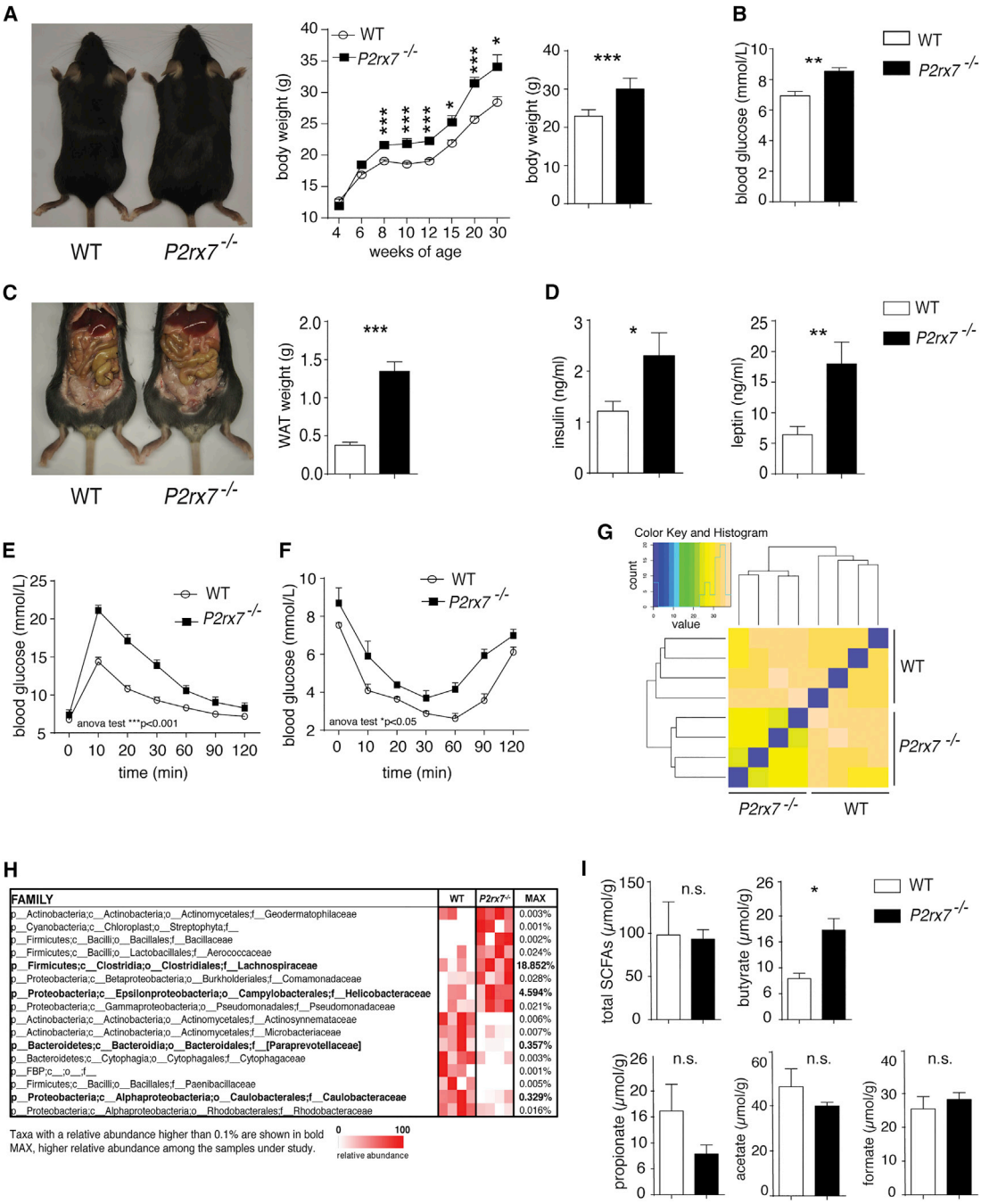

Figure 1. Alterations of Metabolic Parameters and Microbiota Composition in *P2rx7*$^{-/-}$ Mice

(A–F) *P2rx7*$^{-/-}$ and WT littermates, weight gain in WT and *P2rx7*$^{-/-}$ mice, and body weight (n = 20) (A) and blood glucose concentration (n = 20) (B) at 9 weeks. Also shown are representative abdomens and statistics of WAT weights (n = 20) (C). Serum insulin and leptin concentrations (n = 20) are shown (D) as well as glucose homeostasis determined by GTT (E) and ITT (F) in WT and *P2rx7*$^{-/-}$ mice (n = 5).

(G) Similarity in mouse microbiota by Euclidean distances between cecal samples from WT and *P2rx7*$^{-/-}$ mice based on the taxonomic assignment at family rank. Dendrograms show the Euclidean distances between cecal samples, and the matrix colors are proportional to the observed distances.

(H) Heatmap of bacterial families in cecal microbiota that discriminate WT from *P2rx7*$^{-/-}$ mice. Families were selected according to $p < 0.1$ with two-tailed unpaired Student's t test. Each line represents one family, and each column represents an individual mouse. Mean relative abundances of families detected in WT and *P2rx7*$^{-/-}$ mice and the p value for each family are shown. Operational taxonomic units (OTUs) with a relative abundance higher than 0.1% in at least one sample are shown in bold.

(I) SCFA quantification in cecum content of WT and *P2rx7*$^{-/-}$ mice (n = 5).

Means ± SEM are shown, and Mann-Whitney test (A–D, and I) and two-way ANOVA (E and F) were used. *$p < 0.05$, **$p < 0.01$, ***$p < 0.001$; n.s., non-significant.

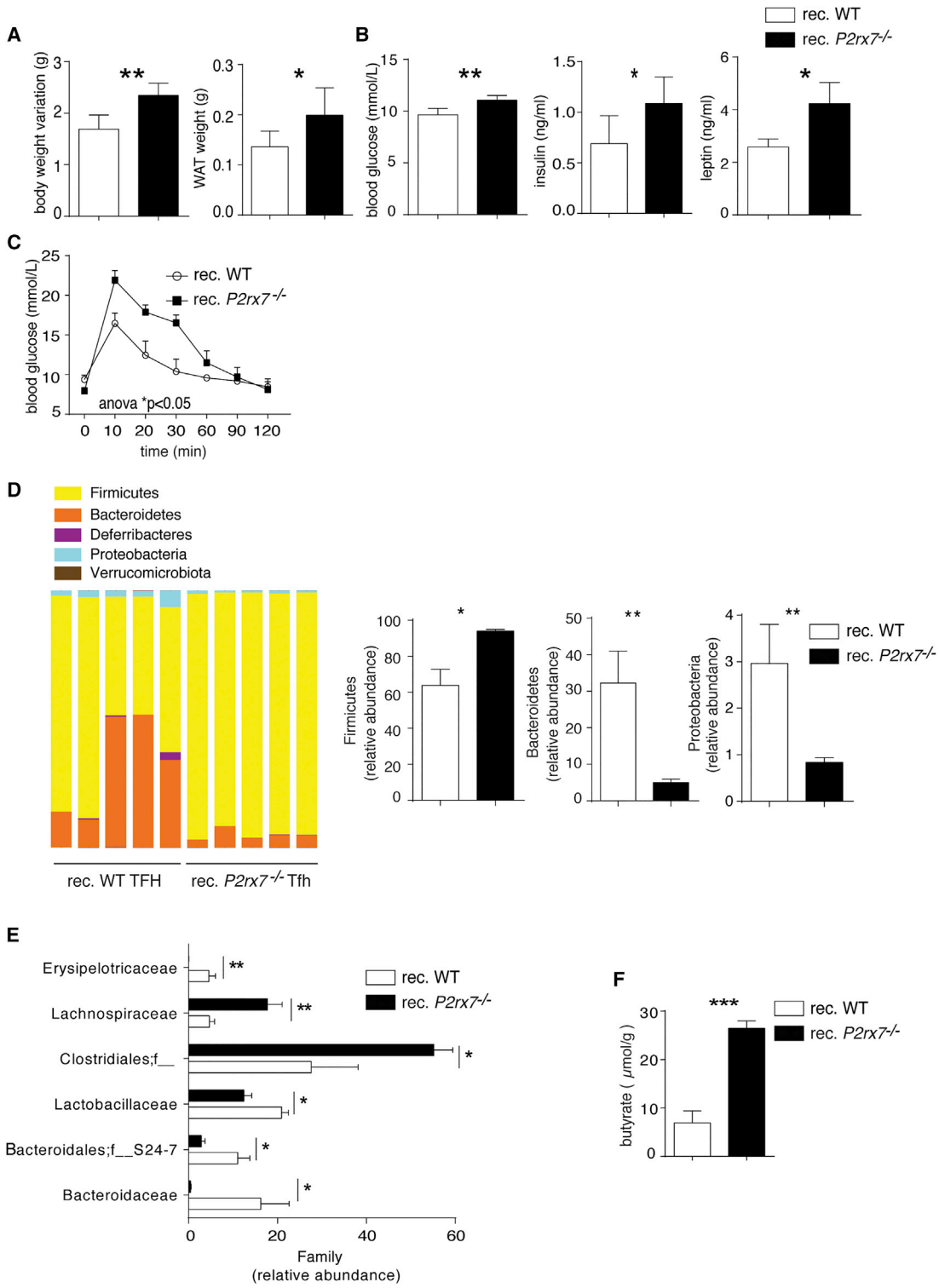

Figure 2. Cell-Intrinsic Role of Tfh Cells in Regulating Glucose Metabolism

(A–C) Body weight variation and WAT weight (A); blood glucose, insulin, and leptin levels (B); and GTT (C) in *Cd3e*$^{-/-}$ mice reconstituted with WT or *P2rx7*$^{-/-}$ Tfh cells (n = 5).

(D and E) Phylum (D) and family (E) relative abundances in *Cd3e*$^{-/-}$ mice reconstituted with WT or *P2rx7*$^{-/-}$ Tfh cells (n = 5).

(F) Butyrate quantification in cecum content of *Cd3e*$^{-/-}$ mice reconstituted with WT or *P2rx7*$^{-/-}$ Tfh cells (n = 5).

Means ± SEM are shown, and Mann-Whitney test (A, B, and D–F) and two-way ANOVA (C) were used. *p < 0.05, **p < 0.01, ***p < 0.001.

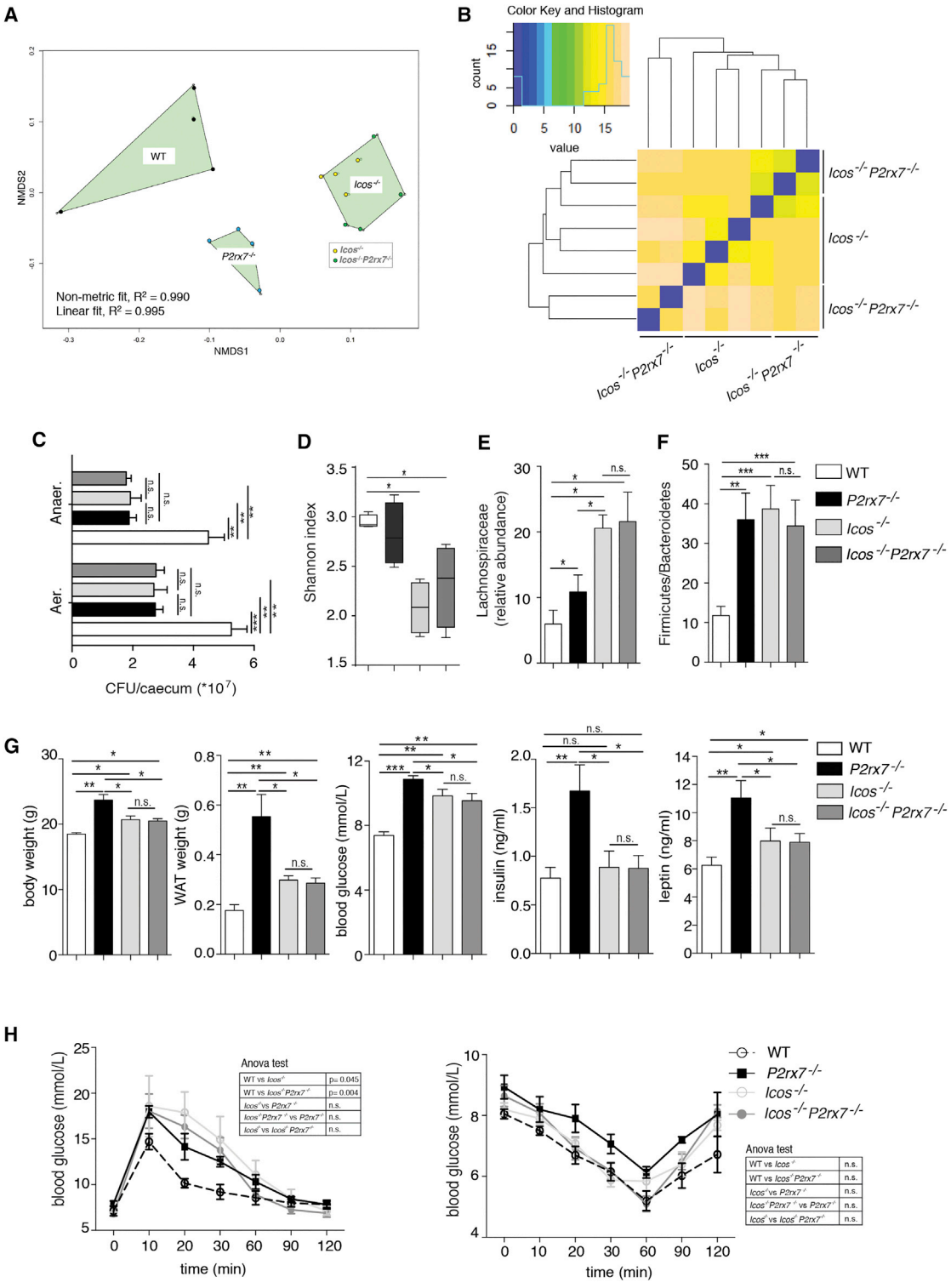

Figure 3. Crucial Role of Tfh Cells in Shaping Commensal Microbiota Composition

(A) Similarity among cecal microbiota through non-metric multidimensional scaling (NMDS) based on an unweighted Unifrac dissimilarity matrix.

(B) Euclidean distances inferred on taxonomic assignment at family rank between cecal samples from *Icos*$^{-/-}$ and *Icos*$^{-/-}$*P2rx7*$^{-/-}$ mice.

(C) Statistical analysis of CFUs of aerobic and anaerobic bacteria recovered from the ceca of WT, *P2rx7*$^{-/-}$ (n = 10), *Icos*$^{-/-}$, and *Icos*$^{-/-}$*P2rx7*$^{-/-}$ mice (n = 5).

(D) Box and whisker plots of the Shannon diversity index at the bacterial family level in WT, *P2rx7*$^{-/-}$, *Icos*$^{-/-}$, and *Icos*$^{-/-}$*P2rx7*$^{-/-}$ mouse cecal samples (n = 4).

(legend continued on next page)

does not influence the enhanced IgA response (Figure S4A). Notably, culture of aerobic and anaerobic bacteria from the cecum revealed the significant reduction of colony-forming units (CFUs) in samples from ICOS-deficient and *P2rx7*$^{-/-}$ mice (Figure 3C), suggesting that deregulated IgA might impair the expansion of the cecal microbial community.

The overall microbiota compositions of *Icos*$^{-/-}$ mutants clustered together by β-diversity analysis and were well separated from WT- and *P2rx7*$^{-/-}$-derived samples (Figure 3A). *Icos*$^{-/-}$ also co-clustered with *Icos*$^{-/-}$*P2rx7*$^{-/-}$ mice for microbiota composition in a hierarchical clustering analysis (Figure 3B). These data indicate that *Icos* deletion (i.e., lack of Tfh cells) causes drastic changes in the gut microbial taxonomic structure. Moreover, α-diversity was significantly reduced in ICOS-deficient animals, supporting the importance of Tfh cell activity in generating a diverse microbiome (Kawamoto et al., 2014; Figure 3D). The reduction of microbial biodiversity in *Icos*$^{-/-}$-associated microbiota was reflected by depletion of microbial functions through phylogenetic investigation of communities by reconstruction of unobserved states (PICRUSt) prediction of metabolic potential (Langille et al., 2013; Figure S4B). In *Icos*$^{-/-}$ and *Icos*$^{-/-}$*P2rx7*$^{-/-}$ mice, we observed a significant increase in the Lachnospiraceae (Figure 3E) and Firmicutes to Bacteroidetes ratio (Figure 3F) together with significantly increased body and WAT weights, blood glucose, and leptin (Figure 3G). Moreover, glucose tolerance was impaired. Different from *P2rx7*$^{-/-}$ mice, serum insulin and insulin tolerance tests were not altered in both *Icos*$^{-/-}$ and *Icos*$^{-/-}$*P2rx7*$^{-/-}$ mice with respect to WT mice (Figures 3G–3H). Notably, *Icos*$^{-/-}$ and *Icos*$^{-/-}$*P2rx7*$^{-/-}$ mice were characterized by indistinguishable metabolic parameters, ruling out a contribution of P2X7 in ICOS^{-} cells to these phenotypic traits. Altogether, these results underscore the importance of Tfh cells in selecting a proficient microbiota for host glucose homeostasis.

Role of Commensal Microbiota in Altered Glucose Metabolism of *P2rx7*$^{-/-}$ Mice

We treated WT and *P2rx7*$^{-/-}$ mice with vancomycin, ampicillin, and metronidazole (VAM) to deplete most bacterial species present in the gut. As expected, Tfh cells from *P2rx7*$^{-/-}$ mice were relatively resistant to cell death induced by massive release of bacterial ATP by VAM compared with WT cells (Figure S5A). Administration of VAM resulted in a significantly enhanced reduction in body and WAT weights as well as blood glucose in *P2rx7*$^{-/-}$ mice compared with WT littermates (Figures 4A–4C). In addition, serum concentrations of insulin and GTTs of VAM-treated *P2rx7*$^{-/-}$ mice became indistinguishable from their WT counterparts (Figures 4D and 4E). GF *P2rx7*$^{-/-}$ mice at 10 weeks showed analogous body and WAT weights to WT littermates and indistinguishable glucose serum levels as well as tolerance to glucose bolus. Some reduction of insulin serum concentration, albeit not reaching statistical significance, was detected in *P2rx7*$^{-/-}$ mice (Figures S5C and S5D). These data confirm the role of the microbiota in the metabolic phenotype of *P2rx7*$^{-/-}$ mice. To understand whether the changes in the gut microbiota characteristic of *P2rx7*$^{-/-}$ mice were the cause of the observed metabolic phenotype, we transplanted cecal content isolated from *P2rx7*$^{-/-}$ mice into VAM-treated WT animals. Administration of VAM with depletion of the microbiota resulted in significant diminution of Tfh cells; fecal transplant restored Tfh cell abundance. Microbiota isolated from *P2rx7*$^{-/-}$ mice induced a significant increase in Tfh cells compared with autochthonous microbiota (Figure S5B), suggesting that microbiota conditioned by *P2rx7*$^{-/-}$ Tfh cells can amplify the regulation of Tfh cells in a feedforward loop. Mice transplanted with microbiota from *P2rx7*$^{-/-}$ mice gained significantly more weight compared with mice transplanted with bacteria from WT mice (Figure 4F). Moreover, body and WAT weights and blood glucose and insulin concentrations 4 weeks after transplant were all increased in mice harboring bacteria isolated from *P2rx7*$^{-/-}$ mice (Figures 4G and 4H), and tolerance to glucose was significantly impaired (Figure 4I). These results suggest that the gut microbiota associated with *P2rx7*$^{-/-}$ mice has the transmissible capacity to promote the fat deposition and development of metabolic features characteristic of these mutant animals.

ATP Released by Commensals Limits the Secretory IgA Response in the Small Intestine

We directly addressed whether bacterially derived ATP could influence T cell-dependent IgA responses via P2X7. The IgA response to *E. coli* is dependent on Tfh cells in PPs (Lécuyer et al., 2014) and is significantly more effective in *P2rx7*$^{-/-}$ mice (Proietti et al., 2014), suggesting that P2X7 activity can affect the T cell-dependent IgA response. We used a recombinant *E. coli* K-12 strain carrying the pHND10 plasmid, which encodes *phoN2*::HA fusion of *Shigella flexneri*, a periplasmic ATP-diphosphohydrolase (apyrase) (Santapaola et al., 2006; Scribano et al., 2014). Extracellular ATP released concomitantly with *E. coli* growth (Hironaka et al., 2013) was undetectable in cultures of these transformants, indicating that apyrase efficiently abrogated ATP secretion (data not shown). Accordingly, GF mice monocolonized with these bacteria showed significantly reduced ATP in the intestine compared with mice monocolonized with bacteria carrying an empty vector (Figure 4J). Consistent with a role of endoluminal ATP in regulating Tfh cell number and GC reaction in the PPs of the small intestine (Proietti et al., 2014), both Tfh and GC B cells were increased in animals colonized with apyrase-expressing bacteria (Figure 4K), as was *E. coli*-specific IgA in the intestinal fluid (Figure 4L). These data indicate that extracellular ATP released by commensals limits the secretory IgA response in the small intestine.

DISCUSSION

The gut microbiota can affect many aspects of host metabolism, including energy harvesting from nutrients, hepatic lipogenesis,

(E and F) Relative abundance of the Lachnospiraceae family (E) and Firmicutes/Bacteroidetes ratio (F) in the indicated mice (n = 4).
(G) Body and WAT weights and blood glucose, insulin, and leptin concentrations (n = 10).
(H) GTT (left) and ITT (right) in WT (white dots), *P2rx7*$^{-/-}$ (black squares), *Icos*$^{-/-}$ (light gray) and *Icos*$^{-/-}$*P2rx7*$^{-/-}$ (dark gray) mice (n = 10).
Means ± SEM are shown, and Mann-Whitney test (C–G) and two-way ANOVA (H) were used. *p < 0.05, **p < 0.01, ***p < 0.001.

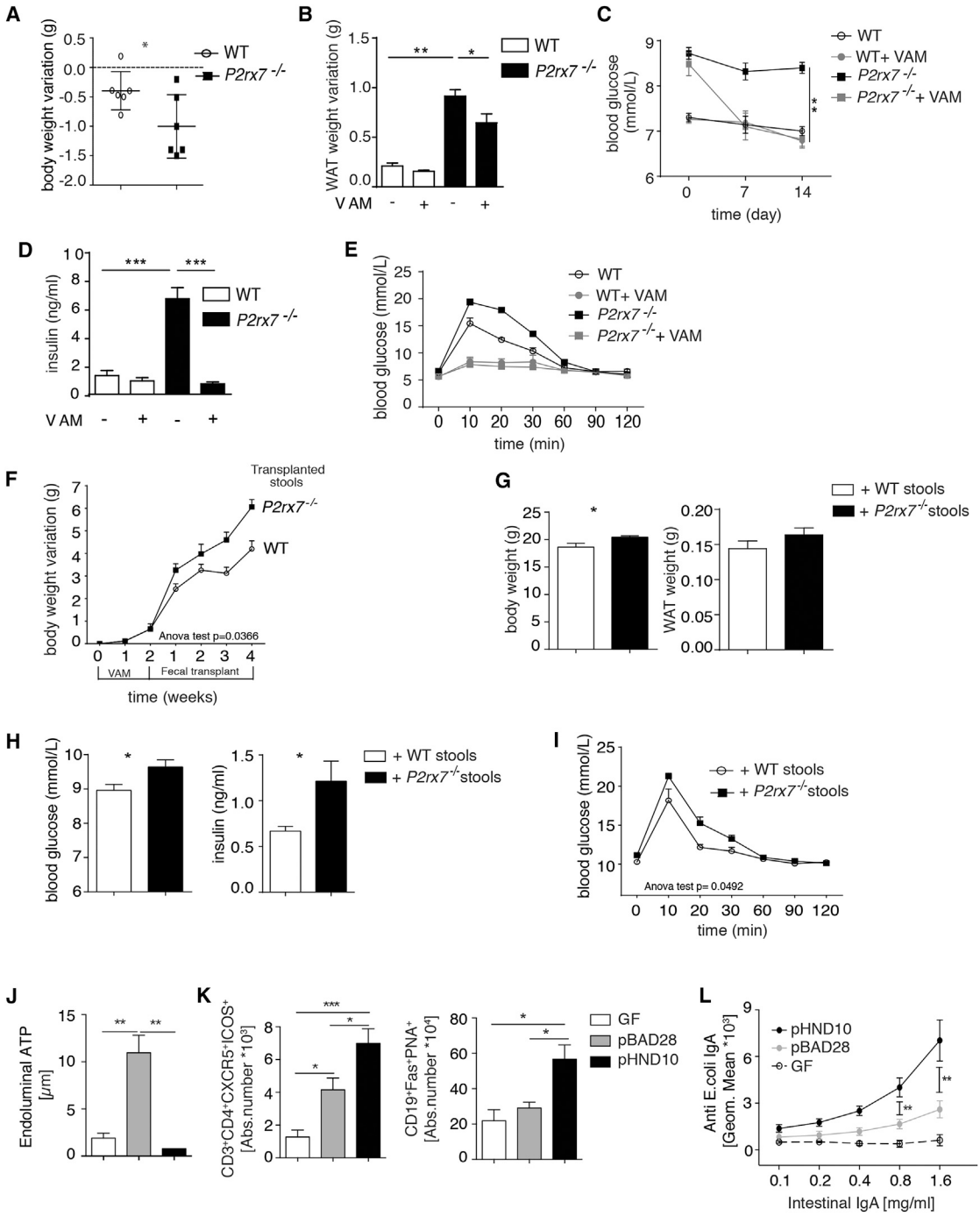

Figure 4. Role of Microbiota of *P2rx7*$^{-/-}$ Mice in Altering Glucose Metabolism

(A–E) Body (A) and WAT (B) weight variation, blood glucose (C) and insulin levels (D), and GTT (E) in WT and *P2rx7*$^{-/-}$ mice after 14 days of VAM (n = 5).

(F–I) Weight gain (F), body and WAT weights (G), blood glucose and insulin (H), and GTT (I) in WT mice transplanted with WT or *P2rx7* $^{-/-}$ microbiota (n = 5).

(J) Concentrations of ATP in ilea from GF mice either non-colonized (GF) or colonized with pBAD28 or pHND10 bearing *E. coli*.

(K) Quantification of Tfh and GC B cells in non-colonized or monocolonized animals as indicated.

(L) Intestinal anti-*E. coli* IgA quantification at fluorescence-activated cell sorting (FACS) (see Experimental Procedures) in GF mice or mice monocolonized with the indicated *E. coli* transformants (n = 5).

Means ± SEM are shown, and Mann-Whitney test (A–D, G, H, and J–L) and two-way ANOVA (E, F, and I) were used. *p < 0.05, **p < 0.01, ***p < 0.001.

and adipose tissue development (Bäckhed et al., 2004; Cox and Blaser, 2013; Turnbaugh et al., 2006). Signaling pathways involved in reciprocal regulation of the adaptive immune system and microbiota to ensure the generation and maintenance of a healthy microbial community are poorly defined. We have shown that regulation of Tfh cell activity by the ATP-gated ionotropic P2X7 receptor contributes to the selection of a beneficial microbiota for glucose metabolism and fat deposition. Interestingly, hypo-functioning P2X7 variants were recently associated with impaired glucose homeostasis in both mice and humans (Todd et al., 2015). We observed that changes in the microbiota by enhanced Tfh cell activity were responsible for metabolic abnormalities and obesity. Previous microbial taxonomy of stool and mucus from *P2rx7*$^{-/-}$ mice did not reveal significant modifications with respect to the WT counterpart (Proietti et al., 2014). Apart from dissimilarities in accurately assigning amplicons to different taxa by the different techniques used for microbiota profiling (Kang et al., 2014), this apparent discrepancy could be due to selective variation in microbiota composition in the ceca of *P2rx7*$^{-/-}$ mice, where diversity of the bacterial ecosystem might be more sensitive to enhanced IgA coating. Bacterial coating by IgA restricts bacterial access to the epithelium and can promote the survival of specific bacteria that affect the intestinal as well as general metabolism (Mantis et al., 2011). Moreover, the diversified microbiota resulting from T-dependent secretory IgA pressure has been suggested to play a pivotal role in promoting the ecological adaptability and speciation potential of mammals (Sutherland et al., 2016).

Release of ATP from commensals limits Tfh cell-dependent helper activity, and abrogation of this release (Figure 4J) or signaling via P2X7 in Tfh cells (Proietti et al., 2014) results in enhanced taxon-specific secretory IgA responses. The results obtained with mice adoptively transferred with Tfh cells indicate that sensing of extracellular ATP by Tfh cells via P2X7 is exclusively responsible for the metabolic alterations observed in *P2rx7*$^{-/-}$ mice. Obesity was associated with an increased ratio of Firmicutes to Bacteroidetes (Cho et al., 2012; Ley et al., 2005; Turnbaugh et al., 2006), which was, in turn, associated with increased concentrations of butyrate in the intestine of obese versus lean mice (Cho et al., 2012; Turnbaugh et al., 2006). This interrelation with possible metabolic relevance might be sensitive to manipulation of the ATP/P2X7 axis in Tfh cells.

Tfh cells are regulated in the PPs by Tfr cells. IgA generated and selected in the presence of Tfr cells coated a larger diversity of bacterial taxa than in their absence. This coating was hypothesized to directly influence the diversity and phylogenetic structure of the intestinal bacterial ecosystem by contributing to the maintenance, rather than elimination, of indigenous bacteria (Kawamoto et al., 2014). We have previously shown that lack of P2X7 results in an increase in Tfh, but not Tfr, cell abundance in the PPs (Proietti et al., 2014). The deregulated activation of Tfh cells in the absence of the concomitant modulation by Tfr cells might result in loss of the controlled diversification of stimulatory bacteria that were hypothesized to promote a self-regulatory loop important for host-bacterial mutualism (Kawamoto et al., 2014). Defective Tfr activity as well as lack of Tfh cells (*Icos*$^{-/-}$ mice) resulted in a higher Firmicutes-to-Bacteroidetes ratio and expansion of bacteria belonging to Lachnospiraceae analogous to mice with P2X7-deficient Tfh cells. These results indicate that regulated GC reaction profoundly affects host metabolism by shaping a proficient microbiota. The lack of sensitivity of PP Tfh cells to endoluminal ATP compromises the host metabolism, thereby suggesting that ATP in the gut acts as an inter-kingdom signaling molecule ensuring the establishment of a healthy relationship between microbiota, the adaptive immune response, and systemic homeostasis.

EXPERIMENTAL PROCEDURES

Mice

All animal experiments were performed in accordance with the Swiss Federal Veterinary Office guidelines and as authorized by the Cantonal Veterinary Office. C57BL/6J, *P2rx7*$^{-/-}$ (B6.129P2-*P2rx7*^{tm1Gab}/J), *Icos*$^{-/-}$, and *Cd3e*$^{-/-}$ mice were bred in the specific pathogen-free (spf) facility at the Institute for Research in Biomedicine Switzerland.

Adoptive Transfer of Tfh Cells

$CD4^+CD8^-CXCR5^+ICOS^+$ cells from pooled PPs of WT or *P2rx7*$^{-/-}$ mice were sorted on a FACSAria. Eight-week-old *Cd3e*$^{-/-}$ mice were injected intravenously (i.v.) with 1×10^5 Tfh cells. Recipient mice were sacrificed 4 weeks after reconstitution.

Microbiota Transplantation

Eight-week-old C57BL/6J mice were gavaged for 2 weeks with vancomycin (1.25 mg), ampicillin (2.5 mg), and metronidazole (2.5 mg) in 200 μL PBS and then gavaged for 3 days with fresh cecal content (200 μL) collected from donor mice and resuspended in PBS (0.01 g/mL).

GTT, ITT, Serum Insulin, and Leptin Quantification

Animals were fasted for 12 hr (GTT) or 6 hr (ITT) and then received an intraperitoneal (i.p.) injection of glucose (2 g/kg of body weight) or insulin (0.6 U/kg). Blood glucose was monitored for 120 min using a glucometer on samples collected from the tip of the tail vein. Insulin and leptin were quantified by ELISA.

Taxonomic Analysis of Microbiota

For the evaluation of intestinal microbiota, the bacterial microbiota of cecal samples from WT, *P2rx7*$^{-/-}$, *Icos*$^{-/-}$, and *Icos*$^{-/-}$*P2rx7*$^{-/-}$ mice has been investigated by sequencing the V5–V6 hypervariable regions of the 16S rDNA gene by using the Illumina MiSeq platform. The prokaryotic composition of the tested samples has been assessed by bioinformatic analysis of metagenomic amplicons (BioMaS) on the paired end (PE) reads generated by Illumina MiSeq sequencing. In experiments with adoptive transfer of Tfh cells, microbial V5 and V6 regions were sequenced on the Ion Torrent PGM (personal genome machine) system using a 316v2 chip and analyzed using QIIME V1.8.0. Operational taxonomic units (OTU) were generated using uclust and a 97% identity threshold. Taxonomy assignment was performed by blasting representative OTU sequences against the latest Greengenes database.

Statistical Analysis

The displayed data are representative of at least three independent experiments. Results were analyzed using the nonparametric Mann Whitney test, Student's unpaired t test, and two-way ANOVA with Bonferroni post-test analysis. Results are presented as mean ± SEM. Values of $p < 0.05$ were considered statistically significant. For statistical analyses of microbiota, R statistic software (version 3.1.2) was used. Differences between the effects on microbiota composition were evaluated by analyzing the data with nonparametric Wilcoxon Mann-Whitney test with Benjamini-Hochberg correction, using paired data when possible, with which we could decide whether the

population distributions were identical without assuming them to follow the normal distribution.

ACCESSION NUMBERS

The accession numbers for the sequences reported in this paper are SRA: SRP099819 and ENA: PRJEB19531 (for adoptive transfer of Tfh cells).

SUPPLEMENTAL INFORMATION

Supplemental Information includes Supplemental Experimental Procedures and five figures and can be found with this article online at http://dx.doi.org/10.1016/j.celrep.2017.02.061.

AUTHOR CONTRIBUTIONS

F.G., L.P., and M.P. designed the experiments. L.P. performed most experiments. M.P., C.E.F., and T.R.J. performed experiments. A.M.D., C.M., and M.G. performed 16S metagenomic sequencing. L.M. and D.C. performed gas chromatography for SCFA quantification, G. Pellegrini performed the histological analysis. A.M. and G.D.N. performed the liver gene expression analysis. G.G., B.F., G. Pesole, M.B.G., and S.G. contributed bioinformatic analyses. M.G. and K.D.M. generated GF mice. D.S. and M.N. contributed *E. coli* transformants. F.G. and L.P. analyzed data and wrote the paper with contributions from G.G. and S.G.

ACKNOWLEDGMENTS

We thank David Jarrossay (Institute for Research in Biomedicine) for cell sorting and Teresa De Filippis, Claudia Lionetti (University of Bari), and Caterina Manzari (Institute of Biomembranes and Bioenergetics) for contributing to 16S metagenomic sequencing. The work was supported by grant 310030_159491 and Sinergia CRSII2_127547 of the Swiss National Science Foundation (SNSF), grant 12A09 of the Novartis Stiftung für Medizinisch-Biologische Forschung, Nano-Tera Project 20NA21_128841, Fondazione Ticinese per la Ricerca sul Cancro, and Fondazione per la Ricerca sulla Trasfusione e sui Trapianti and Converge Biotech (to F.G.). The Ph.D. fellowship of L.P. was supported by Signora Alessandra. C.M. was supported by MD-PhD-Programm SNF323530_158124. K.D.M. is supported by a grant from the SNSF (SNSF310030_134902) and European Research Council (FP/2007-2013) agreement no. 281785.

Received: August 8, 2016
Revised: January 24, 2017
Accepted: February 17, 2017
Published: March 14, 2017

REFERENCES

Bäckhed, F., Ding, H., Wang, T., Hooper, L.V., Koh, G.Y., Nagy, A., Semenkovich, C.F., and Gordon, J.I. (2004). The gut microbiota as an environmental factor that regulates fat storage. Proc. Natl. Acad. Sci. USA *101*, 15718–15723.

Beaucage, K.L., Xiao, A., Pollmann, S.I., Grol, M.W., Beach, R.J., Holdsworth, D.W., Sims, S.M., Darling, M.R., and Dixon, S.J. (2014). Loss of P2X7 nucleotide receptor function leads to abnormal fat distribution in mice. Purinergic Signal. *10*, 291–304.

Bunker, J.J., Flynn, T.M., Koval, J.C., Shaw, D.G., Meisel, M., McDonald, B.D., Ishizuka, I.E., Dent, A.L., Wilson, P.C., Jabri, B., et al. (2015). Innate and adaptive humoral responses coat distinct commensal bacteria with immunoglobulin A. Immunity *43*, 541–553.

Cho, I., Yamanishi, S., Cox, L., Methé, B.A., Zavadil, J., Li, K., Gao, Z., Mahana, D., Raju, K., Teitler, I., et al. (2012). Antibiotics in early life alter the murine colonic microbiome and adiposity. Nature *488*, 621–626.

Cox, L.M., and Blaser, M.J. (2013). Pathways in microbe-induced obesity. Cell Metab. *17*, 883–894.

Dong, C., Juedes, A.E., Temann, U.A., Shresta, S., Allison, J.P., Ruddle, N.H., and Flavell, R.A. (2001). ICOS co-stimulatory receptor is essential for T-cell activation and function. Nature *409*, 97–101.

Duncan, S.H., Barcenilla, A., Stewart, C.S., Pryde, S.E., and Flint, H.J. (2002). Acetate utilization and butyryl coenzyme A (CoA):acetate-CoA transferase in butyrate-producing bacteria from the human large intestine. Appl. Environ. Microbiol. *68*, 5186–5190.

Fagarasan, S., Muramatsu, M., Suzuki, K., Nagaoka, H., Hiai, H., and Honjo, T. (2002). Critical roles of activation-induced cytidine deaminase in the homeostasis of gut flora. Science *298*, 1424–1427.

Hironaka, I., Iwase, T., Sugimoto, S., Okuda, K., Tajima, A., Yanaga, K., and Mizunoe, Y. (2013). Glucose triggers ATP secretion from bacteria in a growth-phase-dependent manner. Appl. Environ. Microbiol. *79*, 2328–2335.

Kang, S.S., Jeraldo, P.R., Kurti, A., Miller, M.E., Cook, M.D., Whitlock, K., Goldenfeld, N., Woods, J.A., White, B.A., Chia, N., and Fryer, J.D. (2014). Diet and exercise orthogonally alter the gut microbiome and reveal independent associations with anxiety and cognition. Mol. Neurodegener. *9*, 36.

Kawamoto, S., Maruya, M., Kato, L.M., Suda, W., Atarashi, K., Doi, Y., Tsutsui, Y., Qin, H., Honda, K., Okada, T., et al. (2014). Foxp3(+) T cells regulate immunoglobulin a selection and facilitate diversification of bacterial species responsible for immune homeostasis. Immunity *41*, 152–165.

Langille, M.G., Zaneveld, J., Caporaso, J.G., McDonald, D., Knights, D., Reyes, J.A., Clemente, J.C., Burkepile, D.E., Vega Thurber, R.L., Knight, R., et al. (2013). Predictive functional profiling of microbial communities using 16S rRNA marker gene sequences. Nat. Biotechnol. *31*, 814–821.

Lécuyer, E., Rakotobe, S., Lengliné-Garnier, H., Lebreton, C., Picard, M., Juste, C., Fritzen, R., Eberl, G., McCoy, K.D., Macpherson, A.J., et al. (2014). Segmented filamentous bacterium uses secondary and tertiary lymphoid tissues to induce gut IgA and specific T helper 17 cell responses. Immunity *40*, 608–620.

Ley, R.E., Bäckhed, F., Turnbaugh, P., Lozupone, C.A., Knight, R.D., and Gordon, J.I. (2005). Obesity alters gut microbial ecology. Proc. Natl. Acad. Sci. USA *102*, 11070–11075.

Littman, D.R., and Pamer, E.G. (2011). Role of the commensal microbiota in normal and pathogenic host immune responses. Cell Host Microbe *10*, 311–323.

Macpherson, A.J., and Harris, N.L. (2004). Interactions between commensal intestinal bacteria and the immune system. Nat. Rev. Immunol. *4*, 478–485.

Mantis, N.J., Rol, N., and Corthésy, B. (2011). Secretory IgA's complex roles in immunity and mucosal homeostasis in the gut. Mucosal Immunol. *4*, 603–611.

Meehan, C.J., and Beiko, R.G. (2014). A phylogenomic view of ecological specialization in the Lachnospiraceae, a family of digestive tract-associated bacteria. Genome Biol. Evol. *6*, 703–713.

Proietti, M., Cornacchione, V., Rezzonico Jost, T., Romagnani, A., Faliti, C.E., Perruzza, L., Rigoni, R., Radaelli, E., Caprioli, F., Preziuso, S., et al. (2014). ATP-gated ionotropic P2X7 receptor controls follicular T helper cell numbers in Peyer's patches to promote host-microbiota mutualism. Immunity *41*, 789–801.

Santapaola, D., Del Chierico, F., Petrucca, A., Uzzau, S., Casalino, M., Colonna, B., Sessa, R., Berlutti, F., and Nicoletti, M. (2006). Apyrase, the product of the virulence plasmid-encoded phoN2 (apy) gene of Shigella flexneri, is necessary for proper unipolar IcsA localization and for efficient intercellular spread. J. Bacteriol. *188*, 1620–1627.

Scribano, D., Petrucca, A., Pompili, M., Ambrosi, C., Bruni, E., Zagaglia, C., Prosseda, G., Nencioni, L., Casalino, M., Polticelli, F., and Nicoletti, M. (2014). Polar localization of PhoN2, a periplasmic virulence-associated factor of Shigella flexneri, is required for proper IcsA exposition at the old bacterial pole. PLoS ONE *9*, e90230.

Shroff, K.E., Meslin, K., and Cebra, J.J. (1995). Commensal enteric bacteria engender a self-limiting humoral mucosal immune response while permanently colonizing the gut. Infect. Immun. *63*, 3904–3913.

Sutherland, D.B., Suzuki, K., and Fagarasan, S. (2016). Fostering of advanced mutualism with gut microbiota by immunoglobulin A. Immunol. Rev. *270*, 20–31.

Todd, J.N., Poon, W., Lyssenko, V., Groop, L., Nichols, B., Wilmot, M., Robson, S., Enjyoji, K., Herman, M.A., Hu, C., et al. (2015). Variation in glucose homeostasis traits associated with P2RX7 polymorphisms in mice and humans. J. Clin. Endocrinol. Metab. *100*, E688–E696.

Turnbaugh, P.J., Ley, R.E., Mahowald, M.A., Magrini, V., Mardis, E.R., and Gordon, J.I. (2006). An obesity-associated gut microbiome with increased capacity for energy harvest. Nature *444*, 1027–1031.

Wei, M., Shinkura, R., Doi, Y., Maruya, M., Fagarasan, S., and Honjo, T. (2011). Mice carrying a knock-in mutation of Aicda resulting in a defect in somatic hypermutation have impaired gut homeostasis and compromised mucosal defense. Nat. Immunol. *12*, 264–270.

Cell Reports, Volume *18*

Supplemental Information

T Follicular Helper Cells Promote a Beneficial Gut Ecosystem for Host Metabolic Homeostasis by Sensing Microbiota-Derived Extracellular ATP

Lisa Perruzza, Giorgio Gargari, Michele Proietti, Bruno Fosso, Anna Maria D'Erchia, Caterina Elisa Faliti, Tanja Rezzonico-Jost, Daniela Scribano, Laura Mauri, Diego Colombo, Giovanni Pellegrini, Annalisa Moregola, Catherine Mooser, Graziano Pesole, Mauro Nicoletti, Giuseppe Danilo Norata, Markus B. Geuking, Kathy D. McCoy, Simone Guglielmetti, and Fabio Grassi

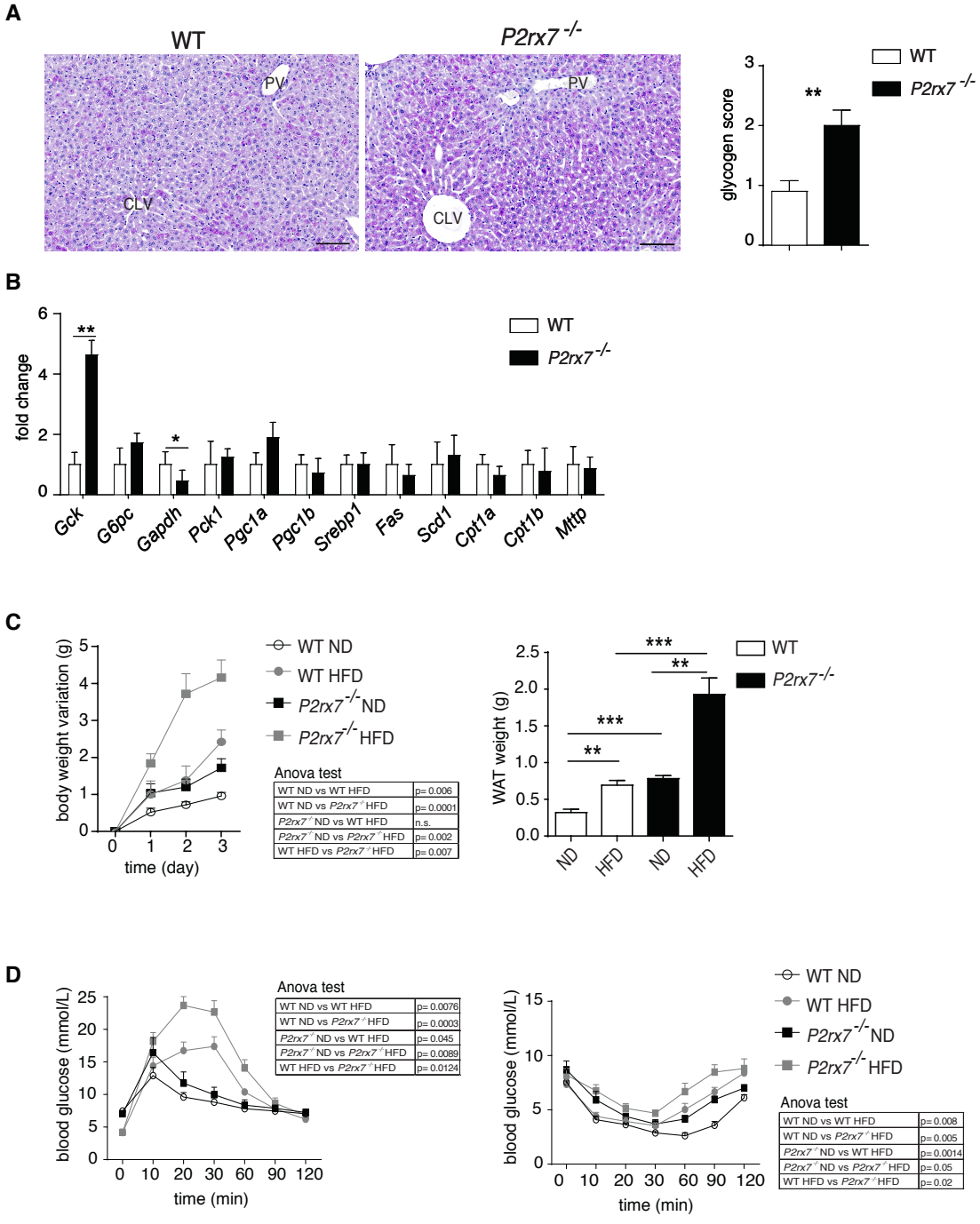

Figure S1. Glycogen accumulation in the liver and enhanced deterioration of glucose metabolism by high-fat diet in *P2rx7*$^{-/-}$ mice, Related to Figure 1 (A) PAS-stained liver sections from *P2rx7*$^{-/-}$ and WT littermates and statistical analysis of glycogen score (see Experimental Procedures). Relative glycogen accumulation is indicated by presence of magenta staining within the hepatocyte cytoplasm (CLV: centrilobular veins, PV: portal veins, scale bar: 100 μm). (B) Hepatic mRNA levels of genes involved in glycolysis (GK, GAPDH), fatty acid catabolism (CPT1a, CTP1b, PGC1α, PCGC1β), fatty acids and lipoprotein synthesis (SREBP1, FAS, SCD1, MTTP). (C) Increase in body weight during 3 weeks of high fat diet (HFD) in WT (grey dot) and *P2rx7*$^{-/-}$ (grey square) mice (n=5); control mice with normal diet (ND) are also shown (left) and WAT weights at 3 wks (right). (D) GTT and ITT after 3 weeks of HFD. Mean ± SEM are shown, Mann-Whitney (A, B and C) and Two-way ANOVA (C, D) tests were used. *p < 0.05, **p < 0.01, ***p < 0.001.

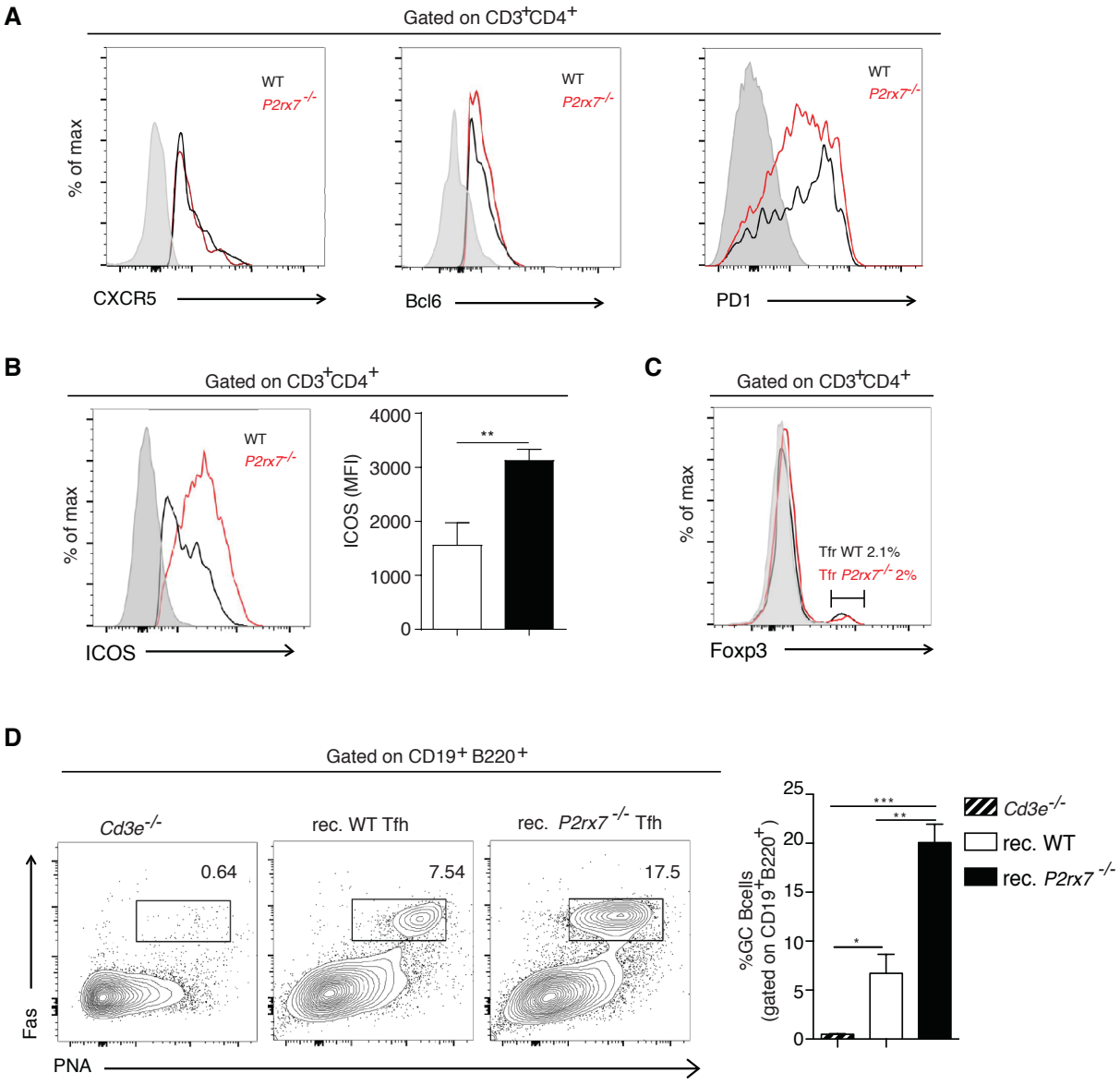

Figure S2. Phenotype of Tfh cells and GC B cells at one month after transfer into *Cd3e*$^{-/-}$ mice, Related to Figure 2. (A) Quantification of Tfh cells in PPs of *Cd3e*$^{-/-}$ mice reconstituted with purified WT or *P2rx7*$^{-/-}$ Tfh cells. (B-D) FACS histograms overlays of gated WT or *P2rx7*$^{-/-}$ CD4 cells isolated from PPs of reconstituted *Cd3e*$^{-/-}$ mice for: (B) CXCR5, Bcl6 and PD1; (C) ICOS with statistical analysis of MFI; (D) Foxp3. (E) Representative contour plots and statistical analysis of Fas^{+}PNA^{+} GC B cells in *Cd3e*$^{-/-}$ mice either non-reconstituted or reconstituted with WT or *P2rx7*$^{-/-}$ Tfh cells. Means ± SEM are shown, Mann-Whitney tests was used. **p < 0.01, ***p < 0.001.

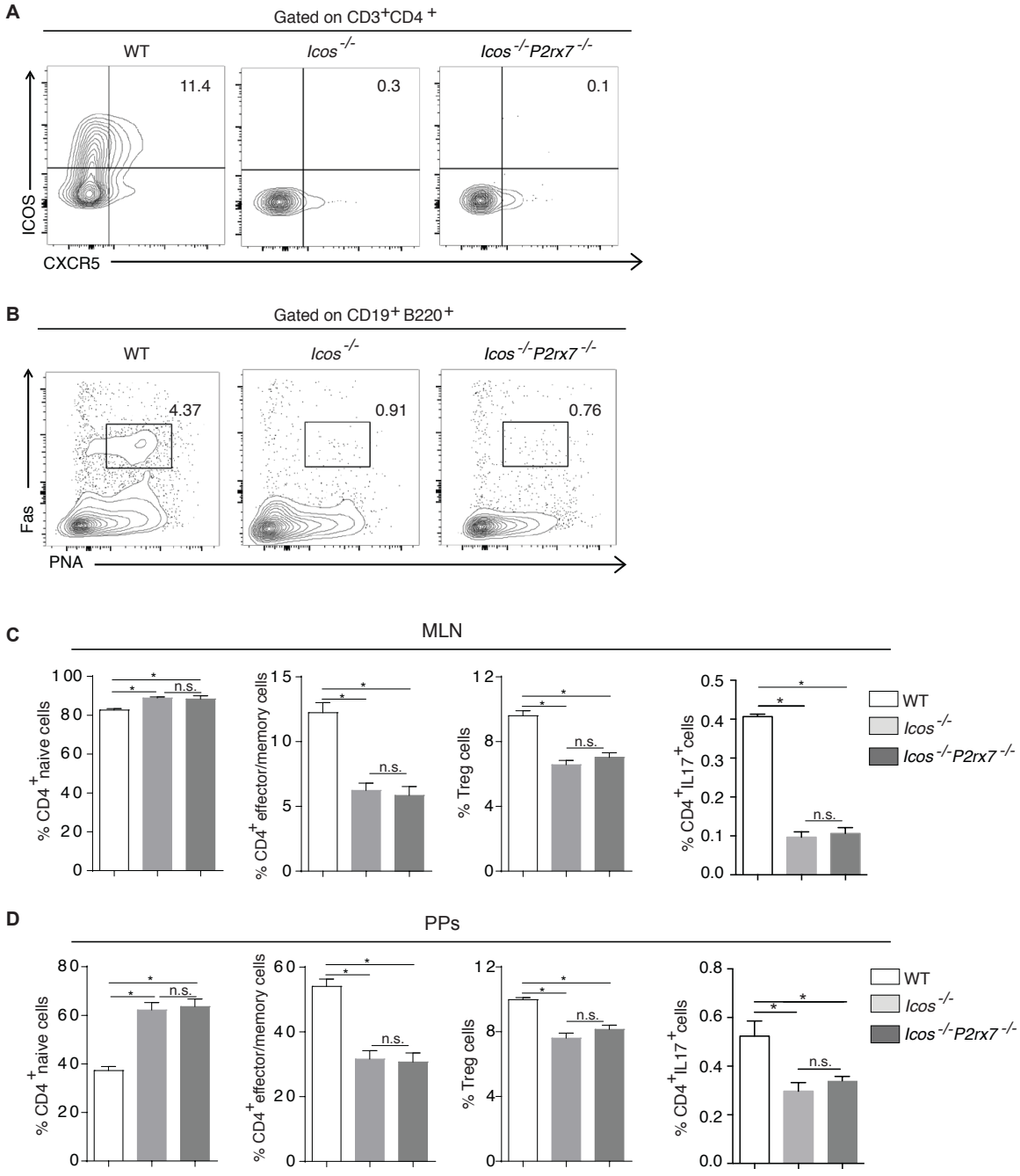

Figure S3. Phenotype of CD4 cells in *Icos*$^{-/-}$ and *Icos*$^{-/-}$*P2rx7*$^{-/-}$ mice, Related to Figure 3. (A) Contour plots of $CD3^+CD4^+$ cells from PPs stained for CXCR5 and ICOS. (B) Contour plots of $CD19^+B220^+$ B cells stained for Fas and PNA. (C, D) Statistical analysis of naïve, effector/memory, Treg and IL-17 secreting CD4 cells in MLN (C) and PPs (D). *$p < 0.05$; n.s., non-significant.

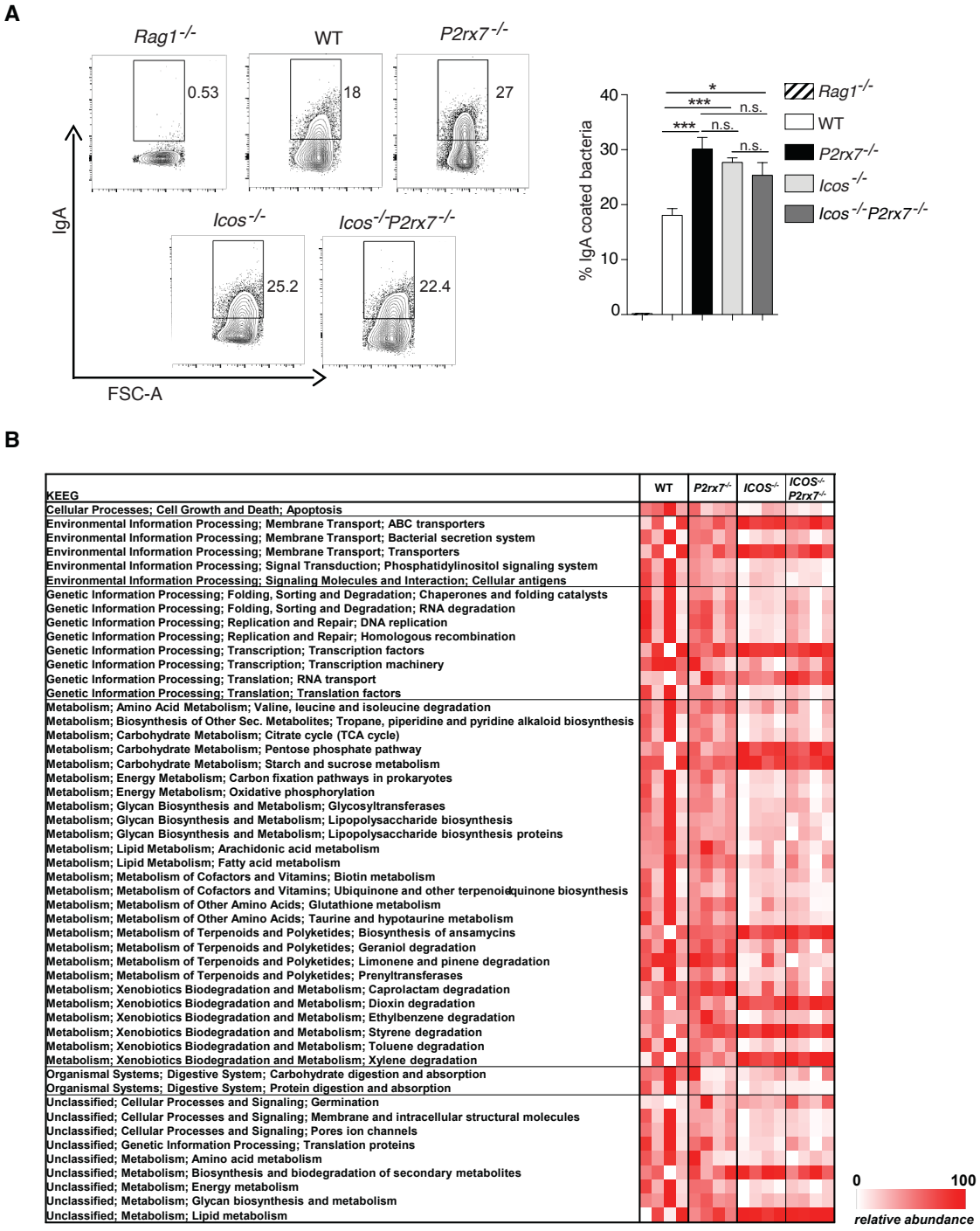

Figure S4. IgA coating in fecal bacteria and Phylogenetic Investigation of Communities by Reconstruction of Unobserved States (PICRUSt), Related to Figure 3. (A) Representative contour plots of IgA coating and forward scatter at FACS of fecal bacteria isolated from the indicated mice with statistical analysis (Mann-Whitney test, n=10). Percentages of positive bacteria in the indicated quadrant are shown. Mean values ± SEM. ***$p < 0.001$, *$p < 0.05$, n.s., non-significant. (B) Heat map of the predicted metabolic potential of caecal microbiota samples discriminating WT, *P2rx7*$^{-/-}$, *Icos*$^{-/-}$ and *Icos*$^{-/-}$*P2rx7*$^{-/-}$ mice. The relative abundances of KEEG categories have been determined through the PICRUSt software (Langille et al., 2013). Color scale: increasing relative abundance from white to red. Each column represents an individual mouse.

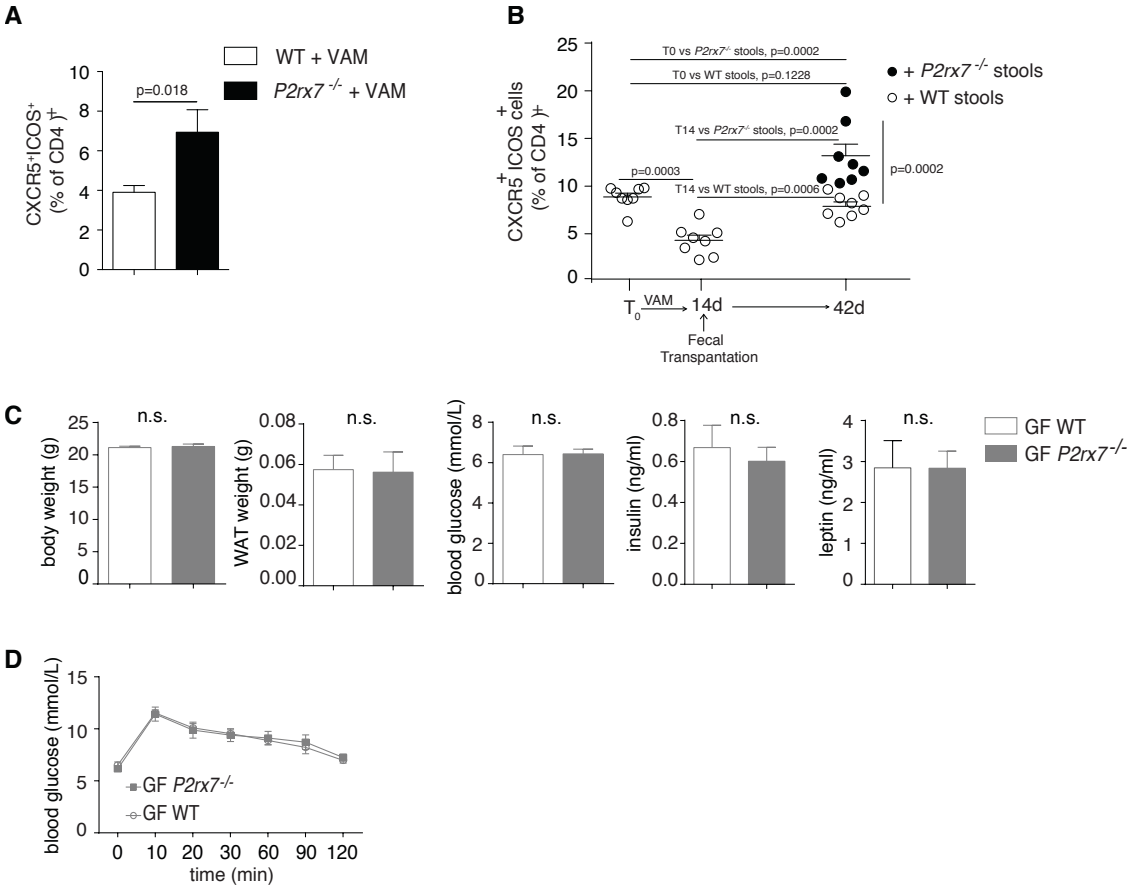

Figure S5. Tfh cells frequency after administration of antibiotics and fecal transplantation, Related to Figure 4. (A) Statistical analysis of Tfh cells in PPs from VAM treated WT or *P2rx7*$^{-/-}$ mice. (B) Statistical analysis of Tfh cells from PPs of WT mice 14 d after administration of VAM and 42 d after transplantation of stools isolated from WT or *P2rx7*$^{-/-}$ mice. (C) Body and WAT weights, blood glucose, serum insulin, leptin levels and (D) GTT in germ-free WT and *P2rx7*$^{-/-}$ mice at 9 wk (n=7). Means ± SEM and p values obtained with Mann-Whitney test are shown. Two-way ANOVA for GTT was not significant.

SUPPLEMENTAL EXPERIMENTAL PROCEDURES

Mice and *in vivo* experiments

C57BL/6J, *P2rx7*$^{-/-}$, *Icos*$^{-/-}$ (Jackson Laboratory), and *Cd3e*$^{-/-}$ (Malissen et al., 1995) mice were bred in specific pathogen-free (spf) facility at the Institute for Research in Biomedicine, Bellinzona, Switzerland. The colony of C57BL/6J, *P2rx7*$^{-/-}$ was maintained onsite with heterozygous breeders and littermates kept in the same cages until weaning at 4 week of age. C57BL/6J and *P2rx7*$^{-/-}$ germ free mice were maintained in flexible film isolators at the Clean Animal Facility, University of Bern, Switzerland. To deplete gut flora, 8 week old C57BL/6J and *P2rx7*$^{-/-}$ mice were treated daily with an antibiotic association containing Metronidazole (2,5 mg), Ampicillin (2,5 mg) and Vancomycin (1,25 mg) (VAM) in 200µl per mouse by oral gavage for 2 weeks. For adoptive transfer of Tfh cells, CD4^{+}CD8^{-}CXCR5^{+}ICOS^{+} cells were sorted at FACSAria from pooled PPs of C57BL/6J or *P2rx7*$^{-/-}$ mice. Eight week old *Cd3e*$^{-/-}$ mice were injected with 1x10^{5} Tfh cells. Recipient mice were sacrificed 4 weeks after reconstitution. All animal experiments were performed in accordance with the Swiss Federal Veterinary Office guidelines and authorized by the Cantonal Veterinary. For body and WAT weights, and blood glucose variations, we show the difference between the initial value and the value obtained at the indicated time points.

Tissue collection and histology

All animals were fasted overnight for 12 h prior to sacrifice. Livers were collected shortly after euthanasia, weighed and fixed in 4% buffered paraformaldehyde (PFA). Paraffin-embedded sections (3-5 µm thick) were routinely stained with hematoxylin and eosin

(H&E) and Periodic Acid Schiff (PAS) reagent for histological evaluation and visualization of glycogen content, respectively. The amount of glycogen was assessed in the PAS-stained sections according to a 0-3 scale modified from Villano et al. (Villano et al., 2013): Grade 0: negligible glycogen levels; Grade 1: patchy glycogen accumulation with a predominant midzonal distribution, affecting less than 30% hepatocytes; Grade 2: uniform glycogen accumulation with a predominant midzonal to centrilobular distribution (31-50%); Grade 3: abundant glycogen accumulation with a panlobular distribution (> 50%).

Liver gene expression

Quantitative PCR analysis of transcripts for gene involved in metabolic pathways in the liver was performed as described (Braccini et al., 2015).

GTT, ITT, serum insulin and leptin quantification.

Animals were fasted for 12 (GTT) or 6 (ITT) h and then received an i.p. injection of glucose (2 g/kg of body weight) or insulin (0.6 U/kg). Blood glucose was monitored for 120 min using a glucometer (Healthpro-x1, Axapharm) on samples collected from the tip of the tail vein. Insulin in serum was quantified using an ELISA kit (High sensitive mouse insulin ELISA kit, Biorbyt Ltd). Leptin was quantified using an ELISA kit (Mouse Leptin Quantikine ELISA Kit, Bio-Techne AG).

SCFA Analysis

An aliquot (100-200 mg) of caecal content was suspended while frozen in 100 μL PBS containing 10 μL stock solution of internal standards (each of the following components at 20 mM: [$^2H_3$]acetate, [$^2H_5$]propionate, and [$^2H_7$]butyrate). After acidification with 10 μl of 37% HCl, SCFAs were extracted twice with 2 ml diethyl ether (Samuel and Gordon, 2006). A 60 μL aliquot of the extracted sample was mixed with 20 μL of *N*-tert-

butyldimethylsilyl-*N*-methyltrifluoracetamide (MTBSTFA, Sigma) at room temperature. An aliquot (2 μL) of the resulting derivatized material was injected into a gas chromatograph coupled with e mass spectrometer. GC-MS analyses were performed by using a Trace GC-Ultra 60 chromatograph coupled with a Trace DSQ mass spectrometer (Thermo Scientific), equipped with a capillary HP-5MS column (Agilent Technologies), and recorded in positive-ion full scan mode with electronic impact for ionization (70 eV) and source temperature 200 °C. Sample solutions (1 μL) were introduced in a splitless mode at 250 °C for the injector and 280 °C for the MS transfer line. Helium at a constant flow-rate of 1 mL/min was used as a carrier gas. The initial oven temperature was held at 80 °C for 5 min, increased to 200 °C at 15°/min and maintained at this value for further 5 min. Data were processed with the aid of the Finnigan Xcalibur™ software system.

Microbiota transplantation

Microbiota transplantation was performed in 8 week old C57BL/6J mice previously treated with VAM for 2 weeks. Fresh caecal content was collected from 5 donor mice (C57BL/6J or *P2rx7*$^{-/-}$*),* resuspended in PBS (0.01 g/ml) and delivered by gavaging in 200 μl for 3 days to recipient animals. Mice were analyzed after 4 weeks.

Antibodies

The following mAbs were purchased from BD Biosciences: biotin conjugated anti-CXCR5 (clone: 2G8, Cat.#: 551960), PE conjugated anti-ICOS (clone: 7E.17G9, Cat.#: 552146). The following mAbs were purchased from Biolegend: PE-Cy7 conjugated anti-CD4 (Clone:GK1.5, Cat.# 100422). Efluo405 conjugated streptavidin was from eBioscience (Cat.#: 48-4317-82).

Cell isolation and adoptive transfer

Single-cell suspensions were prepared from pooled PPs harvested from C57BL/6J or *P2rx7*$^{-/-}$ mice. For adoptive transfer of Tfh cells, CD4^{+}CD8^{-}CXCR5^{+}ICOS^{+}cells were sorted at FACSAria from pooled PPs of C57BL/6J or *P2rx7*$^{-/-}$ mice. Eight week old *Cd3e*$^{-/-}$ mice were injected with 1x10^{5} Tfh cells. Recipient mice were sacrificed 4 weeks after reconstitution.

Fecal IgA Flow Cytometry

For analysis of IgA coated bacteria in flow cytometry fecal samples were collected and homogenized in PBS (0.01 g/ml). The homogenized samples were centrifuged at 400 x g for 5 min to remove larger particles from bacteria. Supernatants were centrifuged at 8'000 x g for 10 min to remove unbound Igs. Bacterial pellets were resuspended in PBS 5% goat serum (Jackson Immunoresearch), incubated 15 minutes on ice, centrifuged and resuspended in PBS 1% BSA for staining with APC conjugated rabbit anti-mouse IgA antibodies (http://www.brookwoodbiomedical.com/ Cat.#: SAB1186, working dilution 1:200). After 30 min incubation, bacteria were washed twice and resuspended in 2% paraformaldehyde in PBS for acquisition at LSRFortessa (BD Biosciences). FSC and SSC parameters in logarithmic mode were used. SYBR Green was added to identify bacteria-sized particles containing nucleic acids.

Taxonomic analysis of microbiota

For the evaluation of intestinal microbiota, the bacterial microbiota of caecal samples from WT, *P2rx7*$^{-/}$, *Icos*$^{-/-}$ *and Icos*$^{-/-}$*P2rx7*$^{-/-}$ has been investigated by sequencing the V5-V6 hypervariable regions of 16S rDNA gene by using the Illumina MiSeq platform as described in Manzari et al. (Manzari et al., 2015). The prokaryotic composition of the

tested samples has been assessed by the BioMaS (Bioinformatic analysis of Metagenomic AmpliconS) pipeline (Fosso et al., 2015) on the paired-end (PE) reads generated by Illumina MiSeq sequencing. The overlapping 2x250 bp PE reads were merged into consensus sequences by using Flash (Magoc and Salzberg, 2011) and sequences shorter than 50nt were removed. Non-overlapping PE reads were further cleaned by removing low-quality regions (quality-score threshold equal to 25) and discarding PE reads containing sequences shorter then 50nt by using Trim-Galore (http://www.bioinformatics.babraham.ac.uk/projects/trim_galore/). In order to minimize the background noise due to host DNA contamination both consensus and non-overlapping denoised PE reads were mapped against a collection of *Mus musculus* genome by using Bowtie2 (Langmead and Salzberg, 2012). Sequences with an identity percentage ≥ 97% were discarded. The retained consensus and unmerged PE reads were compared to the 11.2 release of the RDP II database (Cole et al., 2009) by using Bowtie2. In order to obtain the taxonomic classification, mapping data were filtered according to two parameters: identity percentage (≥ 90%) and query coverage (≥ 70%). The taxonomic data at family level were normalized by converting the raw count in RPM (reads per million) by using the following formula: RPM = assigned reads / (total assigned reads at the rank level/1.000.000). The alpha-diversity index (Shannon Index) was measured by applying the R package phyloseq (McMurdie and Holmes, 2013) on the taxonomic data at family level (Segata et al., 2011). In experiments with adoptive transfer of Tfh cells into *Cd3e*$^{-/-}$ mice, microbial 16S rRNA gene segment spanning the variable V5 and V6 regions was amplified using the barcoded forward primer 5'-*CCA TCT CAT CCC TGC GTG TCT CCG ACT CAG* BARCODE ATT AGA TAC CCY GGT AGT CC-3' in

combination with the reverse primer 5'-*CCT CTC TAT GGG CAG TCG GTG AT* ACG AGC TGA CGA CAR CCA TG-3'. The sequences in italic are Ion Torrent PGM-specific adaptor sequences required for high throughput sequencing. 16S PCR amplicons were gel purified and sequenced on the Ion Torrent PGM system using a 316v2 chip according to the manufacturer's instructions (Life Technologies). At least 10'000 reads were obtained per samples. The microbial profiles were analyzed using QIIME V1.8.0 (Caporaso et al., 2010). Operational taxonomic units (OTU) were generated using uclust and a 97% identity threshold. Taxonomy assignment was performed by blasting representative OTU sequences against the latest Greengenes database.

Colonization of germ-free mice with *E. coli*

E. coli K-12 transformed with pBAD28 or pHND10 were previously described (Scribano et al., 2014). Bacterial suspensions (10^{10} CFUs in 300 µl) were gavaged into the stomach. After 28 days the small intestine was flushed with 10 ml of intestinal wash buffer (PBS, 0.5M EDTA, Soybean trypsin inhibitor, PMSF), spun at 14'000 rpm in a sterile tube and filtered (0.22 µm) to remove any bacteria-sized contaminants. For FACS analysis of anti-*E. coli* IgA, 3ml of LB broth were inoculated with single colonies and cultured overnight at 37°C. Cultures were subsequently centrifuged (3 min at 7'000 rpm), washed 3 times with sterile-filtered PBS, 2% BSA, 0.005% NaN_3 and resuspended at a density of approximately 10^7 bacteria per ml. Intestinal wash and bacteria were then mixed and incubated at 4°C for 1h. Bacteria were washed twice, before being stained with monoclonal FITC-anti-mouse IgA (Southern Biotech, Cat.#: 1040-02). After 1 h incubation, bacteria were washed twice and resuspended in 2% paraformaldehyde in PBS for acquisition on a FACSCanto using FSC and SSC parameters in logarithmic

mode. For each animal analyzed, ELISA was used to determine the total IgA concentration in an undiluted aliquot of the same intestinal wash sample used for surface staining of *E. coli*. This value was used to calculate the total IgA concentration at each dilution of intestinal wash used for FACS analysis of *E. coli* and was plotted against the geometric mean fluorescence obtained in flow cytometry. ATP concentration was evaluated by bioluminescence assay with recombinant firefly luciferase and its substrate D-luciferin according to the manufacturer's protocol (Molecular Probes, Cat.# A22066).

Statistical analysis

The displayed data are representative of at least three independent experiments. Results were analyzed using the nonparametric Mann Whitney test, Student's unpaired t test and two-way ANOVA with Bonferroni post-test analysis. Results are presented as mean ± SEM. Values of $p < 0.05$ were considered statistically significant.

For statistical analyses of microbiota R statistic software (version 3.1.2) was used. Differences between the effects on microbiota composition were evaluated by analyzing the data with non-parametric Wilcoxon-Mann-Whitney test with Benjamini-Hochberg correction, using paired data when possible, with which we could decide whether the population distributions were identical without assuming them to follow the normal distribution. The choice for a non-parametric test derived from the Shapiro-Francia test performed for the composite hypothesis of normality. The p-value was computed from the formula given by Royston (Royston, 1993). Two-tailed unpaired t-test with a cut-off p-value of 0.1 was performed to select bacterial taxa that could evidence differences between study groups in a heatmap. To describe the variation between genotypes, a non-metric multidimensional scaling (NMDS) was performed using "vegan" library in R on

UNIFRAC dissimilarity matrix, supported by ANOSIM analysis of similarities test. Statistical significance was set at $p \leq 0.05$, and the mean differences with $0.05 < p \leq 0.10$ were accepted as trends. Estimation of metabolic potential from 16S rRNA gene sequencing data in caecal and fecal samples was computationally predicted using PICRUSt (phylogenetic investigation of communities by reconstruction of unobserved states) (Langille et al., 2013). PICRUSt profiles were expressed as Kyoto Encyclopedia of Genes and Genomes (KEGG) (Ferrario et al., 2014).

SUPPLEMENTAL REFERENCES

Braccini, L., Ciraolo, E., Campa, C.C., Perino, A., Longo, D.L., Tibolla, G., Pregnolato, M., Cao, Y., Tassone, B., Damilano, F.*, et al.* (2015). PI3K-C2gamma is a Rab5 effector selectively controlling endosomal Akt2 activation downstream of insulin signalling. Nature Communications *6*, 7400.

Caporaso, J.G., Kuczynski, J., Stombaugh, J., Bittinger, K., Bushman, F.D., Costello, E.K., Fierer, N., Peña, A.G., Goodrich, J.K., Gordon, J.I., *et al.* (2010). QIIME allows analysis of high-throughput community sequencing data. Nature Methods *7*, 335-336.

Cole, J.R., Wang, Q., Cardenas, E., Fish, J., Chai, B., Farris, R.J., Kulam-Syed-Mohideen, A.S., McGarrell, D.M., Marsh, T., Garrity, G.M., and Tiedje, J.M. (2009). The Ribosomal Database Project: improved alignments and new tools for rRNA analysis. Nucleic Acids Research *37*, D141-145.

Ferrario, C., Taverniti, V., Milani, C., Fiore, W., Laureati, M., De Noni, I., Stuknyte, M., Chouaia, B., Riso, P., and Guglielmetti, S. (2014). Modulation of fecal Clostridiales

bacteria and butyrate by probiotic intervention with Lactobacillus paracasei DG varies among healthy adults. The Journal of Nutrition *144*, 1787-1796.

Fosso, B., Santamaria, M., Marzano, M., Alonso-Alemany, D., Valiente, G., Donvito, G., Monaco, A., Notarangelo, P., and Pesole, G. (2015). BioMaS: a modular pipeline for Bioinformatic analysis of Metagenomic AmpliconS. BMC Bioinformatics *16*, 203.

Langille, M.G., Zaneveld, J., Caporaso, J.G., McDonald, D., Knights, D., Reyes, J.A., Clemente, J.C., Burkepile, D.E., Vega Thurber, R.L., Knight, R.*, et al.* (2013). Predictive functional profiling of microbial communities using 16S rRNA marker gene sequences. Nature Biotechnology *31*, 814-821.

Langmead, B., and Salzberg, S.L. (2012). Fast gapped-read alignment with Bowtie 2. Nature Methods *9*, 357-359.

Magoc, T., and Salzberg, S.L. (2011). FLASH: fast length adjustment of short reads to improve genome assemblies. Bioinformatics *27*, 2957-2963.

Manzari, C., Fosso, B., Marzano, M., Annese, A., Caprioli, R., D'Erchia, A.M., Gissi, C., Intranuovo, M., Picardi, E., Santamaria, M.*, et al.* (2015). The influence of invasive jellyfish blooms on the aquatic microbiome in a coastal lagoon (Varano, SE Italy) detected by an Illumina-based deep sequencing strategy. Biological Invasions *17*, 923-940.

McMurdie, P.J., and Holmes, S. (2013). phyloseq: an R package for reproducible interactive analysis and graphics of microbiome census data. PloS one *8*, e61217.

Royston, P. (1993). A pocket-calculator algorithm for the Shapiro-Francia test for non-normality: an application to medicine. Statistics in Medicine *12*, 181-184.

Samuel, B.S., and Gordon, J.I. (2006). A humanized gnotobiotic mouse model of host-archaeal-bacterial mutualism. Proceedings of the National Academy of Sciences of the United States of America *103*, 10011-10016.

Scribano, D., Petrucca, A., Pompili, M., Ambrosi, C., Bruni, E., Zagaglia, C., Prosseda, G., Nencioni, L., Casalino, M., Polticelli, F., and Nicoletti, M. (2014). Polar localization of PhoN2, a periplasmic virulence-associated factor of Shigella flexneri, is required for proper IcsA exposition at the old bacterial pole. PloS one *9*, e90230.

Segata, N., Izard, J., Waldron, L., Gevers, D., Miropolsky, L., Garrett, W.S., and Huttenhower, C. (2011). Metagenomic biomarker discovery and explanation. Genome Biology *12*, R60.

Villano, G., Ruvoletto, M., Ceolotto, G., Quarta, S., Calabrese, F., Turato, C., Tono, N., Crescenzi, M., Biasiolo, A., Cattelan, A.*, et al.* (2013). SERPINB3 is associated with longer survival in transgenic mice. Scientific Reports *3*, 3056.